New Journal of Physics
The open–access journal for physics

Magnetic versus non-magnetic doping effects in the Haldane chain compound $PbNi_2V_2O_8$

A Zorko[1,4], D Arčon[1], A Lappas[2] and Z Jagličić[3]

[1] Jožef Stefan Institute, Jamova 39, 1000 Ljubljana, Slovenia
[2] Institute of Electronic Structure and Laser, Foundation for Research and Technology—Hellas, PO Box 1527, 71110 Heraklion, Crete, Greece
[3] Institute of Mathematics, Physics and Mechanics, Jadranska 19, 1000 Ljubljana, Slovenia
E-mail: andrej.zorko@ijs.si

New Journal of Physics **8** (2006) 60
Received 16 February 2006
Published 19 April 2006
Online at http://www.njp.org/
doi:10.1088/1367-2630/8/4/060

Abstract. Study of an impurity-driven phase transition into a magnetically ordered state in the spin-liquid Haldane chain compound $PbNi_2V_2O_8$ is presented. Both macroscopic magnetization as well as ^{15}V nuclear magnetic resonance (NMR) measurements reveal that the magnetic nature of dopants has a crucial role in determining the stability of the induced long-range magnetic order. In the case of non-magnetic (Mg^{2+} doping at the Ni^{2+} sites ($S = 1$), a metamagnetic transition is observed in relatively low magnetic fields. On the other hand, the magnetic order in magnetically (Co^{2+}) doped compounds survives at much higher magnetic fields and temperatures. We attribute this feature to a significant anisotropic impurity–host magnetic interaction. The NMR measurements confirm that the staggered magnetic moments liberated next to the impurity sites, are the reason for the magnetic ordering. In addition, differences in the broadening of NMR spectra and the increase of nuclear spin-lattice relaxation in doped samples indicate an impurity-dependent character for the dominant electron-spin correlations; the latter begin to develop at rather high temperatures with respect to the antiferromagnetic phase-transition temperature.

[4] Author to whom any correspondence should be addressed.

PII: S1367-2630(06)19178-8

Contents

1. Introduction **2**
2. Experimental details **3**
3. Results **4**
3.1. dc magnetization 4
3.2. NMR measurements 6
4. Analysis and discussion **9**
4.1. Frequency shift and broadening of the ^{51}V NMR spectra in doped compounds . 9
4.2. Simulation of the ^{51}V NMR spectra 10
4.3. Electron-spin correlations as detected by the ^{51}V spin-lattice relaxation 13
4.4. Bulk magnetic properties 14
5. Conclusions **15**
Acknowledgments **16**
References **16**

1. Introduction

Highly correlated quantum spin systems exhibit a variety of intriguing magnetic phenomena in reduced dimensions. On numerous occasions in the past, impurities introduced to such systems were successfully employed to reveal the magnetic character of the host materials. The virtue of magnetic doping and the phase boundaries created by non-magnetic dopants is to introduce novel degrees of freedom. Therefore, studying the electronic structure and electron-spin correlations in the vicinity of the impurity sites is essential for understanding the quantum state of the host. For instance, this approach has been widely exploited in the quest for an intimate relation between magnetism and superconductivity in the high-T_c cuprates [1, 2]. Similarly, doping turned out to be an invaluable method for studying the ground state of various transition-metal oxides exhibiting macroscopically coherent ground states. Amongst them, the singlet ground states of $S = 1/2$ spin-Peierls chains [3], spin ladders [4] and Haldane integer-spin chains [5], all show a spin gap in their excitation spectrum.

Common consequences of the non-magnetic impurities embedded in low-dimensional antiferromagnets include enhanced antiferromagnetic (AF) correlations and induced staggered magnetic moments near the impurity sites. These effects manifest in the vicinity of the vacancies in one-dimensional [6] and two-dimensional [7] AF Heisenberg lattices with gapless excitations, as well as in spin-gap systems with robust non-magnetic ground states, including spin-Peierls chains [8, 9], spin ladders [10] and Haldane chains [11, 12]. For this reason, it has been recently argued that the enhanced correlations at short distances have a common origin independent of the long-distance behaviour of the spin correlations. The enhancement can be explained within the so-called 'pruned' resonating-valence-bond picture; it is a consequence of pruning the possible singlet configurations for spins close to the vacancy sites [8, 9]. The staggered magnetic moments were indeed recently observed experimentally in the case of non-magnetically [13, 14] and magnetically [14] doped Haldane chain compound Y_2BaNiO_5. In these studies, exponentially decaying staggered magnetization was detected next to the impurities, with the staggered moments only weakly dependent on the magnetic nature of the dopants.

Furthermore, a rather unexpected feature in different one-dimensional spin-gap systems is the presence of long-range magnetic ordering induced by impurities [3, 4, 15, 16]. The ordering is believed to originate from the impurity-induced staggered moments. These moments are coupled along the chains with an exponentially decaying staggered exchange [12], because the coupling is mediated by virtual excitations of a gapped medium [17]. Deviations from the low dimensionality originating in the crystal structure give rise to interchain coupling with a vital role in providing the three-dimensional magnetic correlations [18]. Recently, there have been a few attempts trying to unify the field of the impurity-induced magnetic ordering. For instance, Mélin [17] highlighted the role of three characteristic temperatures in doped spin-gap systems: namely, the temperature below which intrachain spin correlations begin developing, that related to the typical energy of the staggered exchange, and the Stoner temperature (of the order of the interchain coupling) associated with the development of the three-dimensional magnetic correlations. The magnitude of the latter two parameters was argued to determine whether the impurity-induced long-range ordering (LRO) should be present. There are a number of reports on LRO as a consequence of doping in different spin-gap systems. However, a comprehensive theory capable of 'predicting' the observed transition temperatures and the stability of the induced long-range magnetically ordered states upon external perturbations (such as a magnetic field) seems not to be available yet. Moreover, the influence of the magnetic character of the dopants on the magnetic ordering is particularly vague and prompts further investigation.

The purpose of our study is to provide a further experimental insight into the complex problem of the impurity-induced phenomena pertaining to the magnetism of the spin-gap systems. The emphasis is put on the comparison between magnetic and non-magnetic doping of the Haldane-chain compound $PbNi_2V_2O_8$ possessing chains of Ni^{2+} spins ($S = 1$). In this compound, the nearest-neighbour (*nn*) intrachain exchange coupling $J = 95\,\mathrm{K}$ (in units of k_B) is by far the most dominant magnetic interaction [16]. In present paper, we employ dc magnetization and nuclear magnetic resonance (NMR) techniques to explore the temperature as well as the magnetic-field stability of the impurity-induced long-range magnetic order. In addition, ^{51}V nuclei, weakly coupled to the system of localized electronic moments, act as a local-probe capable of detecting inhomogeneities and reflect dynamics in the electron-spin system. We demonstrate that the magnetic nature of the dopants plays a crucial role in reducing quantum spin fluctuations and thus helps stabilizing the magnetic order in the Haldane chains.

2. Experimental details

All the samples used in this investigation were prepared according to the same solid-state reaction procedure, reported before [19]. The resulting polycrystalline powders can be addressed as solid solutions, since the Mg^{2+} ($S = 0$) and Co^{2+} ($S = 3/2$) substitutions for Ni^{2+} ions are randomly distributed. Phase purity of the samples was verified by powder x-ray and neutron diffractometry [19]–[21], which revealed that the effect of the impurities on the average crystal structure is minor.

Bulk dc magnetic measurements were performed with a Quantum Design SQUID magnetometer. Field-cooled runs were performed between room temperature and 2 K in static magnetic fields of 0.1 and 5 T. ^{51}V NMR measurements were conducted by standard pulsed NMR techniques in an external magnetic field of 6.34 T, in the temperature range $4.2\,\mathrm{K} < T < 300\,\mathrm{K}$. Typical width of applied $\pi/2$ pulses was 6 μs. Due to the rather broad NMR spectra, the spectral

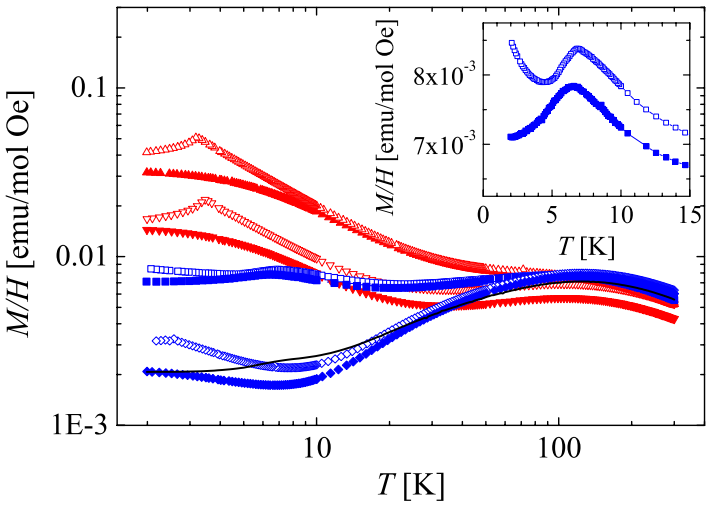

Figure 1. The temperature dependence of the dc magnetization in $PbNi_2V_2O_8$ (——), non-magnetically doped $PbNi_{1.88}Mg_{0.12}V_2O_8$ (▽, ▼) and $PbNi_{1.76}Mg_{0.24}V_2O_8$ (△, ▲), as well as magnetically doped $PbNi_{1.98}Co_{0.02}V_2O_8$ (◇, ♦) and $PbNi_{1.92}Co_{0.08}V_2O_8$ (□, ■) measurements undertaken in magnetic field of 0.1 T (open symbols) and 5 T (full symbols and the solid line). The inset shows a decrease of the low-temperature peak position with increased field in the $PbNi_{1.92}Co_{0.08}V_2O_8$ compound.

width of such pulses was insufficient to reliably detect the full spectra even at room temperature. For this reason, the NMR spectra were obtained in frequency-sweep experiments from the amplitude of the Hahn-echo-detected signals. ^{51}V spin-lattice relaxation was investigated with a saturation–recovery method by employing long comb of pulses.

3. Results

3.1. dc magnetization

The $PbNi_2V_2O_8$ compound undergoes a phase transition from the spin-liquid Haldane ground state into a long-range magnetically ordered state upon doping [16]. The AF nature of the observed ordering was confirmed by the presence of additional Bragg peaks in the neutron diffraction patterns below a characteristic Néel temperature T_N [19]. The ordering can also be detected by dc magnetization measurements, which show a pronounced maximum in the dc magnetization at a temperature coinciding with the phase transition. Such measurements are presented in figure 1 for the two Mg-doped, $PbNi_{1.88}Mg_{0.12}V_2O_8$ and $PbNi_{1.76}Mg_{0.24}V_2O_8$, and the two Co-doped compounds, $PbNi_{1.98}Co_{0.02}V_2O_8$ and $PbNi_{1.92}Co_{0.08}V_2O_8$. In the case of the non-magnetic doping, the phase transition in an external magnetic field of 0.1 T is observed at 3.4 and 3.2 K for $PbNi_{1.88}Mg_{0.12}V_2O_8$ and $PbNi_{1.76}Mg_{0.24}V_2O_8$, respectively, in accordance with the previous measurements [21, 22]. T_N is shifted to 7.1 K in the magnetically doped $PbNi_{1.92}Co_{0.08}V_2O_8$ compound. On the other hand, the transition in the lightly doped $PbNi_{1.98}Co_{0.02}V_2O_8$ compound is found around 2.6 K, similarly to that reported previously [23].

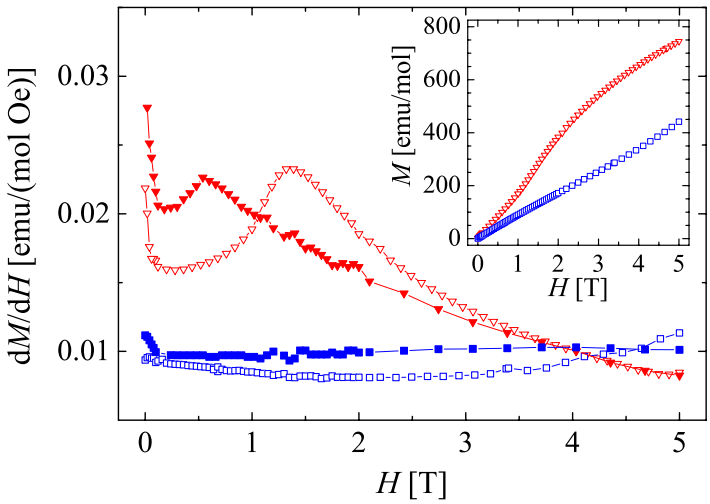

Figure 2. The derivative of the magnetization curves for $PbNi_{1.88}Mg_{0.12}V_2O_8$ (▽) and $PbNi_{1.92}Co_{0.08}V_2O_8$ (□) measured at 2 K as well as at 3.2 and 6.9 K for the case of Mg-doping (▼) and Co-doping (■), respectively. The inset shows the magnetization curves at 2 K.

The magnitude of the impurity-induced low-temperature dc magnetization depends substantially on the magnetic nature of the dopants. This can be attributed to the magnetic coupling between the impurity and the impurity-liberated spins [24]. A quantitative description of this phenomenon has been obtained by considering the impurity–host AF coupling in Co-doped samples ($J_{i-h} = 14$ K) and the effective ferromagnetic coupling between spins neighbouring a particular impurity site ($\tilde{J}' \approx -2$ K). These two are responsible for the existence of low-energy spectral weight of spin excitations, inside the spin gap of the pristine compound [24].

Another feature of the magnetization measurements makes clear distinctions between magnetic and non-magnetic doping in the investigated Haldane compound. Namely, in the case of Mg-doping the peak in the dc magnetization disappears upon increasing the static magnetic field from 0.1 to 5 T. On the other hand, when increasing the field in $PbNi_{1.92}Co_{0.08}V_2O_8$ the peak is only slightly displaced to 6.5 K (inset of figure 1). The latter observation together with the significantly increased T_N in this material indicate enhanced stability of the magnetic order in the cobalt doped samples. The disappearance of the phase transition in relatively low magnetic fields of only a few tesla has been reported before for lightly Mg-doped compounds [25], as well as for the heavily doped $PbNi_{1.76}Mg_{0.24}V_2O_8$ [19]. Based on dc and ac susceptibility results, a field-induced metamagnetic transition has been suggested to be the origin of this behaviour [19]. Now, a similar response is also found in the $PbNi_{1.88}Mg_{0.12}V_2O_8$ sample. More specifically, within the magnetically ordered phase the field dependence of the magnetization curve exhibits a pronounced inflection point (see inset to figure 2), typical of the second-order phase transition from the antiferromagnetically ordered to the paramagnetic (PM) phase [26]. Such transition can be recognized to occur around 1.4 T at 2 K, corresponding to the peak in the derivative of the magnetization curve, as shown in figure 2. The critical field is then expected to be lowered towards zero when the temperature approaches T_N [26], which is in line with the experiment showing the decrease of the critical field to the value of 0.5 T at 3.2 K (figure 2) and follows the experimental behaviour, thoroughly inspected for the case of $PbNi_{1.76}Mg_{0.24}V_2O_8$ [19].

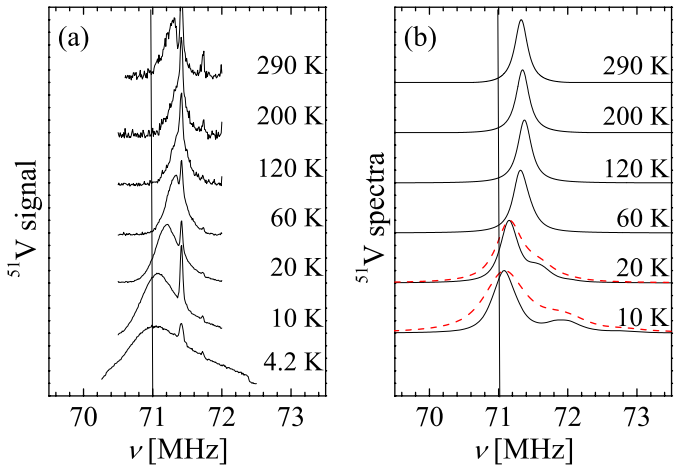

Figure 3. The collection of (a) measured and (b) simulated ^{51}V NMR spectra in $PbNi_{1.88}Mg_{0.12}V_2O_8$. Simulations based on the assumption of temperature-independent homogeneous broadening (——) as well as temperature-dependent broadening (- - - -) are shown.

On the other hand, in $PbNi_{1.92}Co_{0.08}V_2O_8$, a linear dependence of the magnetization is detected in the magnetically ordered state in the whole field range up to 5 T at temperatures close to T_N as well as far below it (figure 2). The curvature of the magnetization curve is slightly enhanced above 4 T at 2 K; however, it seems that even the magnetic field of 5 T is still appreciably lower than the critical one, which could destroy the magnetic order at that temperature. Evidently, the antiferromagnetism in Co-doped samples persists to much higher magnetic fields than in the Mg-substituted materials. NMR results presented in the following sections provide additional support of this observation.

3.2. NMR measurements

We have already reported ^{51}V ($I = 7/2$) NMR measurements on the pristine $PbNi_2V_2O_8$ compound as well as on its Mg-substituted derivatives [27]. At room temperature, the NMR absorption spectra of both Mg-doped samples look qualitatively the same as those of the pristine compound. The linewidth of the latter is virtually temperature independent [27]. On the other hand, the temperature evolution of the spectra in Mg-doped compounds is significant, as shown in figures 3(a) and 4(a). We focus our attention on the broad component of the spectra. A sharp resonance at 71.72 MHz is due to the presence of ^{63}Cu nuclei around our NMR probe. Similarly, the additional narrow component at 71.42 MHz, observed in both Mg-doped samples, is also neglected in the following analysis, because it shows no indications of coupling between the detected nuclei and the electron-spin system [27].

The NMR spectra can be explained by the Hamiltonian

$$\mathcal{H} = \mathcal{H}_Z + \mathcal{H}_Q + \mathcal{H}_{hf} + \mathcal{H}_{cs}, \tag{1}$$

where the first term corresponds to the Zeeman energy of ^{51}V nuclear spins $\mathbf{I}_i$ in the external magnetic field $\mathbf{H}_0$, the second term $\mathcal{H}_Q$ represents the quadrupole coupling of nuclear quadrupole moments with electric field gradients, the hyperfine term $\mathcal{H}_{hf}$ originates from the transferred

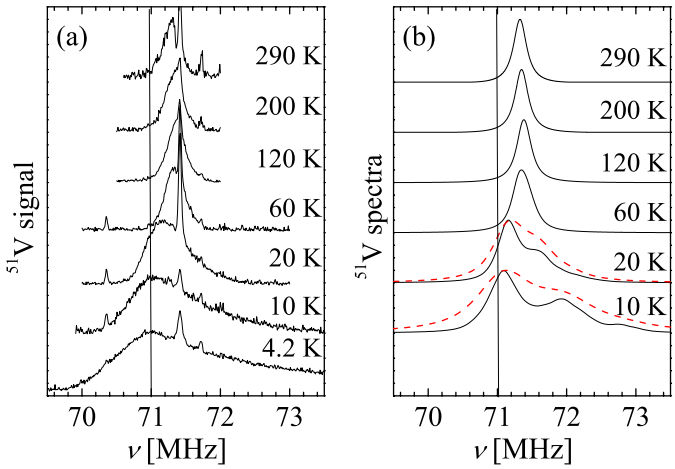

Figure 4. The ^{51}V NMR spectra (a) measured and (b) simulated for the case of $PbNi_{1.76}Mg_{0.24}V_2O_8$. As in the previous figure, simulations based on temperature-independent (——) and temperature-dependent (- - - -) broadening are presented.

hyperfine coupling of vanadium nuclear spins with the surrounding nickel electron spins $\mathbf{S}_j$, and $\mathcal{H}_{cs}$ corresponds to the chemical-shift Hamiltonian. The broad structure of the spectra observed at room temperature originates from the quadrupole coupling with the consecutive satellite transitions displaced by $\nu_Q \approx 80\,\text{kHz}$ [28]. On the other hand, a pronounced broadening of the central transition $(-1/2 \rightarrow 1/2)$ is due to the anisotropy of the chemical-shift tensor [28]. Furthermore, the isotropic part of the transferred hyperfine interaction plays the dominant role in determining the NMR shift. This fact is clearly manifested in the gap-like behaviour of this parameter, which scales with the bulk uniform susceptibility of the parent compound [28].

The standard $VOCl_3$ compound was utilized in order to evaluate the ^{51}V NMR frequency shift. Its ^{51}V NMR spectrum was found at $\nu_L^{dia} = 70.974\,\text{MHz}$. The measured frequency shift in the $PbNi_2V_2O_8$ sample is a combined contribution, namely, that of the isotropic part of the transferred hyperfine interaction and the isotropic part of the chemical-shift tensor. As a result, the Larmor frequency of exactly $\nu_L^0 = 71.0\,\text{MHz}$, corresponding to the pristine compound at 4.2 K, can be used for setting the reference of a zero PM shift. Namely, at such low temperatures the spin susceptibility on the Haldane spin system should be diminished due to its activated behaviour. The value ν_L^0 is marked in our figures displaying the NMR spectra by vertical lines.

When lowering the temperature the spectra of the Mg-doped compounds exhibit a pronounced broadening, in contrast to the parent compound. We have previously speculated that this experimental finding should be a precursor effect of the three-dimensional magnetic ordering in both Mg-doped compounds [27]. In this paper, we offer a quantitative description of the broadening effect. The rationalization is based on the temperature-dependent magnitude of the impurity-induced staggered moments and the development of the three-dimensional correlations between them.

Contrary to the case of the non-magnetic Mg^{2+} doping, magnetic Co^{2+} dopants have a completely different impact on the evolution of the ^{51}V NMR spectra. As shown in figure 5(a), in $PbNi_{1.92}Co_{0.08}V_2O_8$ the spectra exhibit less pronounced broadening with decreasing temperature. They, however, exhibit a drastic change in their width and appearance (two-peak structure) below

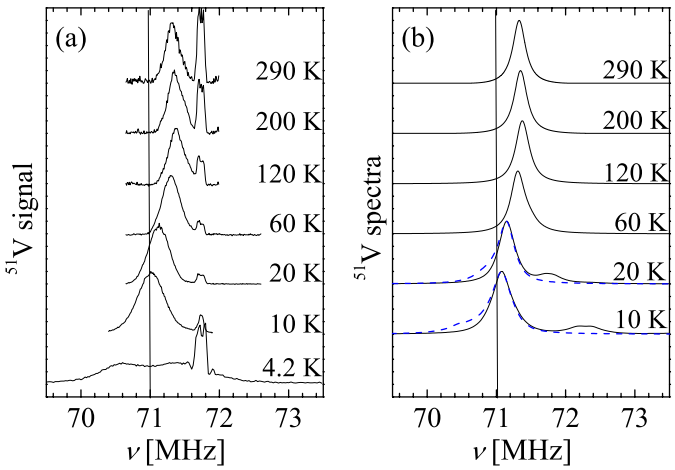

Figure 5. The temperature evolution of (a) measured and (b) simulated ^{51}V NMR spectra in $PbNi_{1.92}Co_{0.08}V_2O_8$. The simulations correspond to PM behaviour (——) and AF correlations (- - - -) impurity and impurity-liberated spins.

6 K, signalling the transition into the magnetically ordered state [28]. The broadening effect is even more reduced in the case of the $PbNi_{1.98}Co_{0.02}V_2O_8$ compound (see next section). Broader NMR spectra in the non-magnetically doped compounds than in the magnetically doped ones seems to be counterintuitive. Magnetic impurities would be expected to couple more efficiently to the vanadium nuclei in contrast to the spin-vacant magnesium sites. Thus, at least close to the phase-transition temperature the Co^{2+} impurities should contribute significantly to the appearance of the NMR spectra due to effective slowing-down of the electron-spin fluctuations.

To get a further insight into the temperature evolution of the electron-spin correlations, we also performed ^{51}V NMR spin-lattice relaxation measurements. At lower temperatures, a pulse-length limitation prevented us from being able to saturate the whole (broad) NMR lines in the doped samples. However, the relaxation was strictly measured at the centre of gravity of the corresponding lines. The saturation–recovery curves were fitted by the stretch-exponential form $M_z(t) = M_0(1 - r\exp[-(t/T_1)^{\alpha}])$. The exponent $\alpha = 0.6(1)$ reflects a multi-exponential nature of the magnetization recovery, typical for quadrupole-split resonances. It displayed only minor temperature and sample dependence.

Due to the strong transferred hyperfine coupling, the spin-lattice relaxation is expected to be caused mainly by transverse electron-spin fluctuations [29, 30]. When the temperature is lowered a rather diverse behaviour is observed among the studied compositions (figure 6). The monotonic decrease of the parameter $(T_1T)^{-1}$ with decreasing temperature in the parent compound is characteristic of the Haldane-gap excitations [31]. On the other hand, the low-temperature up-turn in all the doped samples gives a clear indication of the developing electron-spin correlations (*vide infra*). A rather surprising observation for the parameter $(T_1T)^{-1}$ in the Mg-doped samples is that it deviates from that in the pristine sample from much higher temperatures than in Co-doped samples (figure 6). At the same time, the increase in its magnitude is much more moderate in the non-magnetically doped compounds. Similarly to the bulk magnetic measurement, it is also the NMR results that postulate the impurity-dependent nature of the electron-spin correlations.

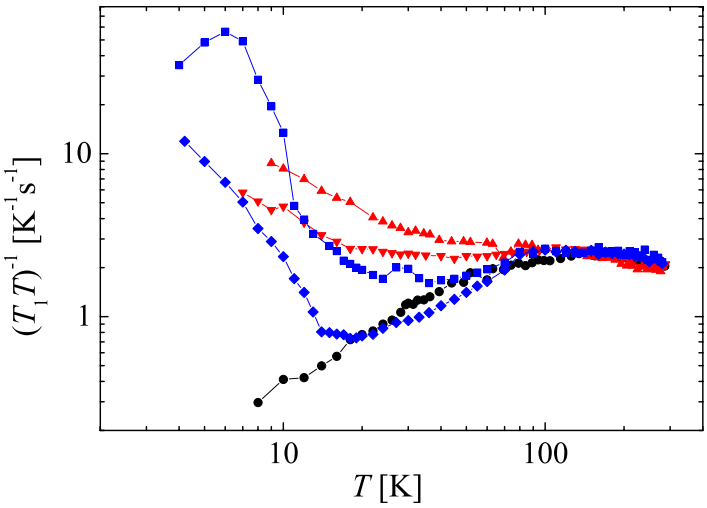

Figure 6. The temperature dependence of the ^{51}V NMR spin-lattice relaxation rate (divided by temperature) in the parent $PbNi_2V_2O_8$ compound (●), the non-magnetically doped $PbNi_{1.88}Mg_{0.12}V_2O_8$ (▼), $PbNi_{1.76}Mg_{0.24}V_2O_8$ (▲) and the magnetically doped $PbNi_{1.98}Co_{0.02}V_2O_8$ (♦), $PbNi_{1.92}Co_{0.08}V_2O_8$ (■) derivatives.

4. Analysis and discussion

4.1. Frequency shift and broadening of the ^{51}V NMR spectra in doped compounds

As already mentioned in the preceding section, the room temperature lineshape of the ^{51}V NMR spectra in the parent as well as in all the doped samples is determined by the quadrupolar Hamiltonian and the anisotropic part of the chemical-shift tensor. In addition, the relatively large shift of the spectra, i.e., $\Delta\nu/\nu_{\mathrm{L}}^0 = 0.4\%$, can be attributed to the transferred hyperfine coupling between the vanadium nuclei and the electronic magnetic moments localized on Ni^{2+} (and impurity) sites,

$$\mathcal{H}_{\mathrm{hf}} = \sum_{i,j} \mathbf{I}_i \cdot \mathbf{A}_{i,j} \cdot \mathbf{S}_j, \tag{2}$$

where the sums run over all the vanadium nuclei ($\mathbf{I}_i$) and over its six nearest-neighbour Ni^{2+} sites ($\mathbf{S}_j$) [20, 28]. Although isolated V^{5+} ions are diamagnetic, they can be addressed as being partially magnetic [32] in the $PbNi_2V_2O_8$ compound. This is due to the imbalance in the closed-shell vanadium orbitals, which is caused by the interaction of vanadium and nickel electrons. As a consequence, the effective transferred hyperfine coupling develops between the ^{51}V nuclear spins and the Ni^{2+} electron spins. In powder samples only the isotropic part of the hyperfine coupling tensor contributes to the NMR shift, allowing an estimate of this parameter,

$$A_{i,j}^{\mathrm{iso}} = \frac{2h\Delta\nu N_{\mathrm{A}} g\mu_{\mathrm{B}}}{6\chi_{\mathrm{mol}} H_0} = 0.17\ \mathrm{mK}. \tag{3}$$

In the above estimation, we used the room temperature value of the molar susceptibility, $\chi_{\mathrm{mol}} = 5.6 \times 10^{-3}$ emu mol^{-1} ($H = 5$ T), as a measure of the average value of the nickel spins,

$\langle S_j^0 \rangle = \chi_{\mathrm{mol}} B_0 / 2 N_{\mathrm{A}} g \mu_{\mathrm{B}}$, in the parent material. The room temperature g-factor value $g = 2.2$ was determined by ESR measurements [33].

Impurity-induced staggered spins $\langle S_j^{\mathrm{i}} \rangle$ in doped Haldane chains are expected to be superimposed on the uniform spin chain. The average spin value at each site is then

$$\langle S_j \rangle = \langle S_j^0 \rangle + \langle S_j^{\mathrm{i}} \rangle . \tag{4}$$

NMR detection of the staggered magnetization near impurity sites has been recently reported for another Haldane chain compound, namely, the Y_2BaNiO_5 [13]. The authors observed additional peaks that were shifted to lower and higher frequencies with respect to the main NMR line of the ^{89}Y nuclei. These lines were attributed to the yttrium nuclei, which were coupled to the staggered moments with exponentially decaying correlations. The temperature dependence of the correlation length was shown to follow the theoretical predictions [34]. Furthermore, the amplitude of the staggered moments, in the case of both non-magnetic Zn^{2+} as well as magnetic Cu^{2+} dopants, was found to exhibit Curie-like dependence for $S = 1/2$ spins [14]. Well-defined chain-end excitations were observed also at temperatures far above the Haldane gap, which was theoretically reproduced by quantum Monte Carlo calculations [35]. This work has provided justification of the use of the simple decomposition for the average spin value, given in equation (4), in a broad temperature range.

Accordingly, the shift of the NMR spectra in doped $bNi_2V_2O_8$ compounds should reflect the impurity-induced contribution to their dc magnetization. figure 7(a) presents the temperature dependence of the centre of gravity (the first moment) for the measured ^{51}V NMR spectra. In the case of the non-magnetic Mg-doping, the expected up-turn in the NMR shift is observed at low temperatures, however, the increase of the dc magnetization in the corresponding temperature regime is much more pronounced (figure 1). The disagreement between the two quantities is even more obvious in the case of the magnetic Co-doping. Here, the impurity contribution to the low-temperature dc magnetization is not reflected at all in the shift of the NMR spectra. Although, at first sight, these observations may suggest that our NMR measurements cannot detect the impurity-induced staggered magnetization, we prove in the subsequent subsection that this is not the case. It is proved to be essential that vacant sites produce shifts towards lower frequencies and that Co^{2+} impurities induce weaker hyperfine coupling to ^{51}V nuclei compared to Mg^{2+} impurities

The linewidth (second moment) of the NMR spectra depends also significantly on the magnetic nature of the dopants (figure 7(b)). The observed broadening with the decreasing temperature is tremendous for the Mg-doped samples. It starts to develop at rather high temperatures with respect to the phase-transition temperature T_{N} in low magnetic fields. On the other hand, the Co-doped samples show a much more moderate broadening in the PM phase and a characteristic critical enhancement of the linewidth in the vicinity of the phase transition. This fact implies a diverse character of the spin correlations determining the low-temperature NMR lineshape in both derivatives. In addition, it is in line with the drastically different stability of the magnetically ordered phase in Mg- and Co-doped $PbNi_2V_2O_8$.

4.2. Simulation of the ^{51}V NMR spectra

Contrary to the ^{89}Y ($I = 1/2$) NMR in Y_2BaNiO_5 [13, 14], the spectra of the ^{51}V nuclei in $PbNi_2V_2O_8$ are quadrupolarly broadened. For this reason, the impurity-induced inhomogeneities of the spin density probed by the ^{51}V nuclei though the transferred hyperfine coupling are hidden

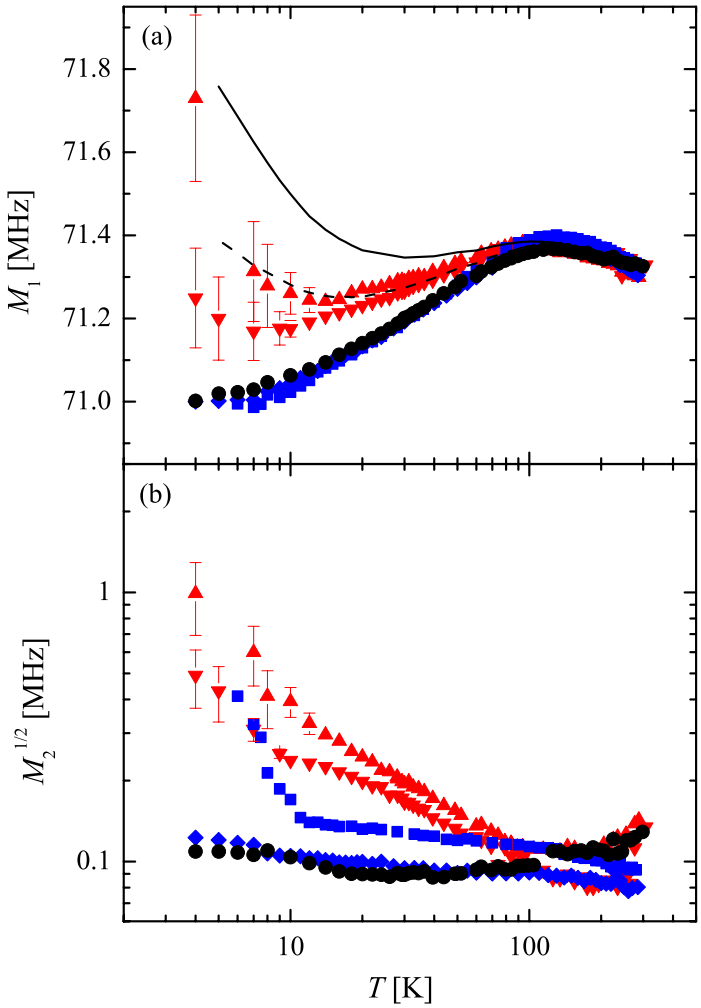

Figure 7. The temperature dependence of the ^{51}V NMR (a) line position and (b) linewidth in $PbNi_2V_2O_8$ (●), $PbNi_{1.88}Mg_{0.12}V_2O_8$ (▼), $PbNi_{1.76}Mg_{0.24}V_2O_8$ (▲), $PbNi_{1.98}Co_{0.02}V_2O_8$ (♦) and $PbNi_{1.92}Co_{0.08}V_2O_8$ (■). The lines correspond to the model explained in the subsection 4.2.

within the spectra at high temperatures. For instance, at room temperature, the $S = 1/2$ degree of freedom that follows the Curie dependence induces according to equation (3) a frequency shift of $\Delta\nu^{\mathrm{i}} = 30\,\mathrm{kHz}$ at the ^{51}V nucleus to which it is coupled. This value should be compared to the width of the room temperature experimental spectra, $2\nu_{\mathrm{Q}} = 160\,\mathrm{kHz}$. At lower temperatures, on the other hand, the impurity-generated features of the NMR spectra are expected to become resolved.

The following simulation procedure was performed in an effort to construct a quantitative picture of the above-mentioned effects. In a finite spin chain ($N = 4096$ spin sites), the impurity positions were randomly distributed, in accordance with a given impurity concentration. The uniform part of the average spin value, $\langle S_j^0 \rangle$, at a certain temperature was deduced from the temperature dependent ^{51}V NMR line position in the pristine compound. The contribution of the staggered moments, $\langle S_j^{\mathrm{i}} \rangle$, was calculated from the position of all impurities. We took into

account the staggered nature of the impurity-induced moments, with the theoretically predicted temperature-dependent correlation length [34] and assumed the magnitude of these moments to be given by the Brillouin function, $S \cdot B_S(g\mu_B SH_0/k_B T)$. In addition, in the case of Co-doping, the impurity spins $S^i = 3/2$, following the Curie dependence, were also taken into consideration. The average spin value interacting with a particular ^{51}V nucleus was then calculated as a sum of four consecutive spins on Ni^{2+} sites in one chain and two spins in its neighbouring chain. Namely, each vanadium nucleus is coupled through an oxygen bridge to four *nn* nickel ions in one chain and to two more *nn* ions in the neighbouring chain. As the vanadium–nickel distances and the bridging angles are similar [20], it is in the first approximation reasonable to assume a common value of the isotropic hyperfine coupling, given in equation (3). On the contrary, a reduced hyperfine coupling was considered for Co^{2+} impurities, $(A_{ij}^{iso})^i = A_{ij}^{iso} J_{i-h}/J$, in accordance with the reduction of the impurity–host exchange J_{i-h} with respect to the *nn* intrachain exchange J [24]. Histograms of the NMR spectra were calculated from the distributions of the average electron-spin values sensed by ^{51}V nuclei. They were then convoluted by a Lorentzian line, with the linewidth corresponding to the room temperature experimental spectra.

4.2.1. Mg-doping. The temperature evolution of the simulated spectra for $PbNi_{1.88}Mg_{0.12}V_2O_8$ and $PbNi_{1.76}Mg_{0.24}V_2O_8$ is presented in figures 3(b) and 4(b), respectively. The solid lines are calculated on the assumption of temperature-independent homogeneous broadening. This corresponds to the case of the parent compound, where the lineshape is predominantly given by the quadrupole Hamiltonian and consequently does not broaden much with decreasing temperature. Although exact agreement with the experimental spectra at lower temperatures is not reached, the impurity-induced shift of a significant portion of the signal towards higher frequencies is in qualitative agreement with the asymmetric broadening of the NMR spectra in both Mg-doped samples. In fact, when a temperature-dependent homogeneous broadening of the lines is assumed, the experimental NMR spectra can be adequately reproduced. This is shown by the dashed lines in figures 3(b) and 4(b). The fits were made down to 10 K because at lower temperatures the assumed Curie dependence should become inappropriate due to the proximity with the temperature region of the AF phase. The predicted spectrum at 10 K is calculated with three times larger homogeneous broadening than the spectrum at room temperature. The enhancement of the homogeneous broadening at temperatures significantly above T_N supports our initial assumptions that the three-dimensional ordering effects should be important already at rather high temperatures [27].

This model can be also used for the prediction of the NMR frequency shifts. The calculated temperature dependence is presented in figure 7(a) by dashed and solid lines, for the cases of $PbNi_{1.88}Mg_{0.12}V_2O_8$ and $PbNi_{1.76}Mg_{0.24}V_2O_8$, respectively. At lower temperatures, the predicted shifts are approximately 1.5 times larger than those measured. This can be a consequence of the simplicity of our model, which takes into consideration the Curie dependence of the staggered moments. Such an assumption is reasonable in the PM phase but close to the Néel temperature a pronounced reduction of the moments is expected. Moreover, also the correlation length should be affected in the vicinity of the magnetically ordered phase. The increased correlation length produces less inhomogeneous distribution of the spins probed by the vanadium nuclei and effectively reduces NMR shifts.

4.2.2. Co-doping. The calculated spectra in the case of the $PbNi_{1.92}Co_{0.08}V_2O_8$ compound are presented in figure 5(b). At temperatures $T \gg J_{i-h}$ (14 K) a PM order for each impurity spin and impurity-induced staggered spins is expected in the external magnetic field. This corresponds to the calculations given by the solid lines. At the other temperature limit, $T \ll J_{i-h}$, AF correlations that produce effective spins $\tilde{S} = 1/2$ at the impurity sites are anticipated. The simulated spectra incorporating such correlations are presented by the dashed lines and agree reasonably with the measurements. The simulations show slight broadening at lower temperatures because of the impurity-generated inhomogeneities in the electron-spin distribution. However, the experimental spectra suggest that also the homogeneous broadening must be enhanced below approximately 20 K. This feature can be understood as a precursor effect due to the proximity with the AF phase transition.

The transition into the magnetically ordered state occurs at approximately 6 K in the magnetic field of 6.34 T. Below this temperature the NMR spectra exhibit strong broadening and the lineshape turns into a symmetric two-peak structure [28], as shown in figure 5(a) at 4.2 K. Such a lineshape can be thought of as a signature of the bipartite spin lattice corresponding to the AF order. However, as the vanadium nuclei sense an average electron-spin value over several sites, non-equivalent Ni–V bonds are required. Different values of the coupling are plausible since the Ni–V distances range from 3.33 to 3.48 Å and the Ni–O–V bridging angles span from 123 to 135° in $PbNi_{1.88}Mg_{0.12}V_2O_8$ [20]; $PbNi_{1.92}Co_{0.08}V_2O_8$ compound has a similar structure.

The observed low-temperature discrepancy between the ^{51}V NMR line position (figure 7(a)) and the corresponding dc magnetization of the $PbNi_{1.92}Co_{0.08}V_2O_8$ sample (figure 1) can be satisfactorily explained within our model. As seen from the simulated NMR spectra (figure 5), AF ordering of each Co^{2+} impurity spin and the neighbouring staggered spins is necessary. In addition, the reduced transferred hyperfine coupling of the vanadium nuclei with cobalt spins with respect to the coupling to nickel spins, is required. The same reasoning can be utilized to explain the severe reduction of the observed broadening in Co-doped samples when compared to the case of Mg-doping. Next, there seems to exist a difference in the intrinsic homogeneous broadening required to reproduce the low-temperature spectra. Surprisingly, this parameter is larger in the case of the non-magnetic doping (not true in the extreme vicinity of T_N). This unexpected observation can be further explored by analysing the NMR spin-lattice relaxation, which in a similar manner to the NMR spectra displays the temperature evolution of the electron-spin correlations.

4.3. Electron-spin correlations as detected by the ^{51}V spin-lattice relaxation

The nuclear spin-lattice relaxation due to the hyperfine interaction, given in equation (2), is related to the transverse components of the electron-spin fluctuations $\delta\mathbf{S} - \langle\mathbf{S}\rangle$ [29, 30]. In the case of the dominant isotropic hyperfine coupling the spin-lattice relaxation rate is determined by the transverse spin correlations $\langle\delta S^+_{\mathbf{q}}(\tau)\delta S^-_{\mathbf{q}}(0)\rangle$, with $\mathbf{q}$ being a wave vector. In the high-temperature approximation, the spin-lattice relaxation is given by [36]

$$\frac{1}{T_1 T} = \frac{k_B}{2\hbar^2}\sum_{\mathbf{q}} A^{iso}_{\mathbf{q}} A^{iso}_{\mathbf{q}} \frac{\chi''(\mathbf{q}, \omega_L)}{\omega_L}, \tag{5}$$

where $A^{iso}_{\mathbf{q}}$ is the Fourier transform of the isotropic hyperfine coupling and $\chi''(\mathbf{q}, \omega_L)$ represents the dissipative part of the transverse dynamical susceptibility.

When approaching the transition into the magnetically ordered state the spin-lattice relaxation is expected to exhibit critical dependence. Such dependence is dictated by the divergent character of the static q-dependent susceptibility in the centre of the AF zone, as well as by the critical slowing down of the spin fluctuations [30]. It is worth noting that the low-temperature increase of the spin-lattice relaxation is much more pronounced than the increase of the static uniform susceptibility reflected in the dc magnetization measurements and the NMR shift. This is because the spin-lattice relaxation detects spin fluctuations at all wave vectors.

The above-mentioned behaviour of the spin-lattice relaxation in Co-doped samples is shown in figure 6. We find that the relaxation rate exhibits strong temperature dependence close to the Néel temperature. In addition, the maximum of $(T_1T)^{-1}$ versus T for $PbNi_{1.92}Co_{0.08}V_2O_8$ at 6 K corresponds nicely with the occurrence of the two-peak structure in the NMR spectra. In contrast, the deviations of the spin-lattice relaxation in Mg-doped samples from the dependence observed in the pristine compound, extend to much higher temperatures. At the same time, the spin-lattice relaxation is suppressed with respect to Co-doping at low temperatures. Although the AF correlations are inhibited by the magnetic field in Mg-doped samples, as observed by the bulk magnetization measurements in 5 T (figure 1), NMR results still show strong spin correlations at some wave vector.

The doping concentrations for both types of dopants are somewhat different in our samples. However, significantly different type of behaviour is observed in the spin-lattice relaxation, reflecting that the electron-spin correlations begin developing in different temperature regions and are evolving much differently with decreasing temperature in the two doping cases. This cannot simply be assigned to different stoichiometry, especially since drastically different behaviour is consistently observed also in other parameters we have presented; the NMR line position, linewidth and the magnetization curves in high magnetic fields reflecting the stability of the magnetic order.

4.4. Bulk magnetic properties

Both the bulk magnetization and the NMR measurements suggest that the magnetically ordered phase is much more robust against the applied magnetic field in the case of the magnetic Co-doping than for the non-magnetic Mg-doping. The metamagnetic transition occurring around 1.4 T at 2 K in the $PbNi_{1.88}Mg_{0.12}V_2O_8$ compound is a consequence of a strong easy-axis single-ion anisotropy D at each Ni^{2+} site [19]. Inelastic neutron scattering (INS) measurements are in support of this behaviour with an extracted $D = -5.2$ K [37].

In general, phase-diagrams of uniaxial Heisenberg antiferromagnets show three distinct phases depending on the value of the single-ion anisotropy and temperature; the PM, the AF and the spin-flop phase. The corresponding theory is available for $S = 1$ systems in the mean-field approximation of the exchange interaction [38]. A direct metamagnetic transition from AF to the PM phase is expected to occur at the critical magnetic field, given at zero temperature as $H_c = zJ_0/g\mu_B$. This is true if $|D| > zJ_0$ (z is the coordination number and J_0 is the exchange constant). The critical field then reduces with temperature.

The investigated spin system is highly inhomogeneous due to its low dimensionality. Therefore, the part of the exchange coupling constant zJ_0 determining the critical field should be taken by the effective coupling providing the three-dimensional magnetic ordering. Due to strong quantum fluctuations, which are important in one-dimensional spin system, the single-ion

anisotropy cannot be simply compared with the exchange coupling parameters. An involved calculation would be rather necessary. However, a rather oversimplified comparison with the Néel temperature, $T_N = 3.4\,K$, yields the zero-temperature critical-field value of the order $H_c \approx k_B T_N / g\mu_B = 2.7\,T$, which is close to our experimental finding, if the limit $T \to 0$ is considered.

The magnetic field above the critical value destroys the three-dimensional magnetic correlations between staggered moments. However, due to the rather low value of the observed critical field, the AF spin correlations within the individual staggered moments should not be affected as they are dictated by the strong *nn* intrachain exchange. Such behaviour was very recently proposed to take place in lightly Mg-doped $CuGeO_3$ compounds, where a field-controlled microscopic separation of the AF and the PM phases was observed [39].

On the other hand, the magnetic ordering in the Co-doped samples survives in magnetic fields even above 6 T, as concluded from our NMR measurements. At low doping concentrations of either magnetic or non-magnetic impurities the indirect staggered exchange $J_s(L) = (-1)^L 0.81 J \exp[-(L-1)/\xi]$ [12], mediated by the gapped Haldane medium, plays the dominant role in determining the stability of the magnetic order. This scenario is confirmed in our case by the strong impurity-concentration dependence of T_N at low doping levels for both types of dopants [23]. On the other hand, at larger substitutions the cross-impurity exchange and the interchain exchange between staggered moments, as weaker exchange coupling mechanisms compared to the indirect staggered exchange, determine the stability of the magnetic order. The improved stability of the magnetic order in Co-doped samples can then be attributed to the significantly enhanced three-dimensional coupling of the impurity-induced staggered moments. The Co^{2+} impurities provide strong coupling between the two neighbouring liberated spin $S = 1/2$ degrees of freedom due to the strong impurity–host exchange, as well as a firmer interchain connection. In addition, due to the strong spin–orbit coupling associated with Co^{2+} [40], an anisotropic exchange is generally observed for these ions. Such anisotropy reduces the spin fluctuations and consequently enhances the stability of the magnetically ordered state. Indeed, doping with Co^{2+} results in by far the highest phase-transition temperatures if compared to other magnetic impurities [23].

Although, conceptionally, the impurity-induced LRO in different spin-gap systems should have a common origin, the system-dependent magnetic properties determining the stability of the ordered state must not be neglected in future theoretical studies. For instance, extensive work on doping the spin-Peierls $CuGeO_3$ compound has shown that the spin of the dopants has only a minor influence on the phase-transition temperature and the spin-flop behaviour. On the contrary, we have demonstrated that the stability of the magnetically ordered state in the $PbNi_2V_2O_8$ Haldane compound is a sensitive function of the magnetic nature of the impurities.

5. Conclusions

We have presented a study of the impurity-induced magnetic ordering in the Haldane compound $PbNi_2V_2O_8$. An intrinsic difference between the effects of the non-magnetic Mg^{2+} and the magnetic Co^{2+} impurities was found. The long-range magnetic order was shown to be destroyed in Mg-doped samples at rather low magnetic fields. However, the AF correlations within the impurity-liberated staggered magnetic moments should survive, as they are governed by the strong *nn* intrachain exchange. On the other hand, the ^{51}V NMR and the bulk magnetization

measurements gave firm evidence for the improved stability of the AF order in the Co-doped samples. These experimental findings were attributed to the enhanced three-dimensional magnetic interactions between localized staggered moments, provided by the substantial anisotropic exchange coupling between impurity and host spins.

The staggered nature of the spins liberated via the substitutions was indirectly explored through the appearance of the ^{51}V NMR spectra. It was shown that the broadening of the spectra as well as the line shift could be associated with the Curie dependence of the impurity-induced staggered magnetic moments; the latter being delocalized on the scale of the theoretically predicted correlation length. Deviations of the model predictions from the experimental results were found only in the vicinity of the Néel-type phase transition. In addition, the NMR measurements offered information about the different character of the electron-spin correlations for both types of doping. In Co-doped materials, the expected critical behaviour of the NMR line broadening and the spin-lattice relaxation was detected at temperatures close to the transition from the PM to the AF state. On the other hand, the pronounced homogeneous broadening of the NMR spectra and the enhanced spin-lattice relaxation in Mg-doped samples was observed to develop at surprisingly high temperatures. These features are present despite the suppression of the AF correlations upon the application of the external magnetic field, as seen by the bulk magnetization measurements. This should be due to enhanced spin correlations positioned at wave vectors outside the centre of the AF zone.

It is envisaged that such a surprising behaviour of the spin correlations will provide a playground that could be further explored by complementary INS measurements. As this experimental technique offers both spectral and spatial information about spin fluctuations, it should uncover additional important aspects of this magnetic-field driven transformation. Shining light on the nature of the spin fluctuations during the metamagnetic transition in the doped Haldane compound $PbNi_2V_2O_8$ is an open issue that warrants further study.

Acknowledgments

We acknowledge the financial support provided by the General Secretariat for Science and Technology (Greece) and the former Ministry of Education, Science and Sport of the Republic of Slovenia through a GR-SLO ‘Joint Research and Technology Program’.

References

[1] Bobroff J, MacFarlane W A, Alloul H, Mendels P, Blanchard N, Collin G and Marucco J-F 1999 *Phys. Rev. Lett.* **83** 4381–4
[2] Hudson E W, Lang K M, Madhavan V, Pan S H, Eisaki H, Uchida S and Davis J C 2001 *Nature* **411** 920–4
[3] Hase M, Terasaki I, Sasago Y, Uchinokura K and Obara H 1993 *Phys. Rev. Lett.* **71** 4059–62
[4] Azuma M, Fujishiro Y, Takano M, Nohara M and Takagi H 1997 *Phys. Rev.* B **55** R8658–R61
[5] Hagiwara M, Katsumata K, Affleck I, Halperin B I and Renard J P 1990 *Phys. Rev. Lett.* **65** 3181–4
[6] Eggert S and Affleck I 1995 *Phys. Rev. Lett.* **75** 934–7
[7] Bulut N, Hone D, Scalapino D J and Loh E Y 1989 *Phys. Rev. Lett.* **62** 2192–5
[8] Martins G B, Laukamp M, Riera J and Dagotto E 1997 *Phys. Rev. Lett.* **78** 3563–6
[9] Laukamp M, Martins G B, Gazza C, Malvezzi A L, Dagotto E, Hansen P M, Lopez A C and Riera J 1998 *Phys. Rev.* B **57** 10755–69
[10] Motome Y, Katoh N, Furukawa N and Imada M 1996 *J. Phys. Soc. Japan* **65** 1949–52

[11] Miyashita S and Yamamoto S 1993 *Phys. Rev.* B **48** 913–9
[12] Sørensen E S and Affleck I 1994 *Phys. Rev.* B **49** 15771–88
[13] Tedoldi F, Santachiara R and Horvatic M 1999 *Phys. Rev. Lett.* **83** 412–5
[14] Das J, Mahajan A V, Bobroff J, Alloul H, Alet F and Sørensen E S 2004 *Phys. Rev.* B **69** 144404
[15] Oosawa A, Ono T and Tanaka H 2002 *Phys. Rev.* B **66** 020405 (R)
[16] Uchiyama Y, Sasago Y, Tsukada I, Uchinokura K, Zheludev A, Hayashi T, Miura N and Böni P 1999 *Phys. Rev. Lett.* **83** 632–5
[17] Mélin R 2000 *Eur. Phys. J.* B **18** 263–73
[18] Inakagi S and Fukuyama H 1983 *J. Phys. Soc. Japan* **52** 3620–9
[19] Lappas A, Alexandrakis V, Giapintzakis J, Pomjakushin V, Prassides K and Schenck A 2002 *Phys. Rev.* B **66** 014428
[20] Mastoraki I, Lappas A, Giapintzakis J, Többens D and Hernández-Velasco J 2004 *J. Solid State Chem.* **177** 2404–14
[21] Mastoraki I, Lappas A, Schneider R and Giapintzakis J 2002 *Appl. Phys.* A (Suppl.) **74** S640–2
[22] Uchinokura K, Uchiyama Y, Masuda T, Sasago Y, Tsukada I, Zheludov A, Hayashi T, Miura N and Böni P 2000 *Physica* B **284–8** 1641–2
[23] Imai S, Masuda T, Matsuoka T and Uchinokura K 2004 *Preprint* cond-mat/0402595
[24] Zorko A, Arčon D, Lappas A and Jagličić Z 2005 *Phys. Rev.* B **73** 104436
[25] Masuda T, Uchinokura K, Hayashi T and Miura N 2002 *Phys. Rev.* B **66** 174416
[26] Stryjewski E and Giorgano N 1977 *Adv. Phys.* **26** 487–650
[27] Arčon D, Zorko A and Lappas A 2004 *Europhys. Lett.* **65** 109–15
[28] Zorko A 2004 *PhD Thesis* University of Ljubljana
[29] Moriya T 1956 *Prog. Theor. Phys.* **16** 23–44
[30] Moriya T 1962 *Prog. Theor. Phys.* **28** 371–400
[31] Sagi J and Affleck I 1996 *Phys. Rev.* B **53** 9188–203
[32] Jaccarino V 1965 *Magnetism* vol IIA, ed G T Rado and H Suhl (New York: Academic) pp**53** 307
[33] Zorko A, Arčon D, Lappas A, Giapintzakis J, Saylor C and Brunel L C 2002 *Phys. Rev.* B **65** 144449
[34] Kim Y J, Greven M, Wiese U and Birgeneau R J 1998 *Eur. Phys. J.* B **4** 291–7
[35] Alet F and Søprensen E S 2000 *Phys. Rev.* B **62** 14116–21
[36] Moriya T 1963 *J. Phys. Soc. Japan* **18** 516–20
[37] Zheludev A, Masuda T, Tsukada I, Uchiyama Y, Uchinokura K, Böni P and Lee S H 2000 *Phys. Rev.* B **62** 8921–30
[38] Vilfan I and Zeks B 1979 *J. Phys. C Solid State Phys.* **12** 4295–309
[39] Glazkov V N, Smirnov A I, Krug von Nidda H-A, Loidl A, Uchinokura K and Masuda T 2005 *Phys. Rev. Lett.* **94** 057205
[40] Pilbrow J R 1990 *Transition Ion Electron Paramagnetic Resonance* (Oxford: Oxford University Press)